

# Importance of Phase Change of Aluminum in Oxidation of Aluminum Nanoparticles

Ashish Rai,<sup>†</sup> Donggeun Lee,<sup>‡</sup> Kihong Park,<sup>†</sup> and Michael R. Zachariah<sup>\*†</sup>

Departments of Mechanical Engineering and Chemistry, University of Maryland, College Park, Maryland 20742, and School of Mechanical Engineering, Pusan National University, Busan 609-735, Korea

Received: November 3, 2003; In Final Form: April 19, 2004

Aluminum nanoparticles have increasingly gained attention because of their potential incorporation in explosive and propellant mixtures. This letter reports on a qualitative study on the oxidation of aluminum nanoparticles containing a passivating oxide coating. Hot-stage transmission electron microscopy (TEM) studies were performed to understand the stability of the oxide coating in nanoaluminum, and oxidation was investigated using a single particle mass spectrometer (SPMS). We find that the oxidation of oxide-coated nanoaluminum coincides with and therefore is presumably initiated by melting of the aluminum core and subsequent mechanical rupture of the oxide coating.

## Introduction

Materials that can store large amounts of chemical energy, and are characterized by a high rate of energy release are termed “energetic materials” and have been used in explosives, propellants and, pyrotechnics. Micron sized aluminum, with a high enthalpy of combustion, is commonly used in rocket propellant formulations. There have been several investigations into the combustion mechanism of micron-sized aluminum particles. Some reports<sup>1,2</sup> suggest that the ignition temperature coincides with the melting point of aluminum oxide. In other studies, researchers<sup>3</sup> used embedded thermocouples and found aluminum ignition at around 2000–2100 K. Still others have found<sup>4–6</sup> that the fracture of oxide shell can take place at a temperature as low as 1300 K, and result in ignition.

The investigations described above focused on micron-sized particles. However, it is well known that fine grained metal particles are highly reactive, and recent interest has focused in fine grained aluminum or “nanoaluminum”. The basic logic being that the rate of energy release will be directly related to the transport of oxidizer to the particle and smaller grains will lead to faster overall energy release.

This in turn led to comparisons of how the burning properties of nanoaluminum might differ from micron-sized aluminum particles. In a recent study it was found that the addition of aluminum nanoparticles can enhance the burning rate of propellants by 5–10 times over conventional aluminum particles.<sup>7</sup> Recently it has also been reported that aluminum nanoparticles formed by electrical wire explosion can ignite, as measured by thermogravimetry (TGA) and differential thermal analysis (DTA), at a temperature as low as 820 K.<sup>8</sup> Most of these recent measurements have been conducted using conventional dynamic thermal techniques such as TGA that require a bulk sample. However, it is known that the response of such methods can be significantly altered by heat and mass transfer effects which are often difficult to account for.<sup>9,10</sup> Ideally an intrinsic analysis of aluminum nanoparticle oxidation would

focus on a single particle without the potential corruption of cooperative particle effects associated with heat and mass transfer to a bulk sample.

This letter presents a qualitative study of the intrinsic reactivity of aluminum nanoparticles and illustrates the importance of aluminum phase change in the oxidation process and the role/stability of the oxide coating. The role of the oxide is of critical importance as it is well known that bare, fine metal particles can be pyrophoric, for which an oxide coating serves as the passivating layer. In this letter we report on the use of hot-stage transmission electron microscopy (HSTEM) and the use of single particle mass spectrometer (SPMS)<sup>9</sup> to characterize the oxidation of nanoaluminum.

## Experimental Methods

For these studies we used commercially available aluminum nanoparticles (Aveka, corp.) dispersed in methanol. TEM analysis indicated that the particles were aggregates of around 150 nm, composed of primary particles of 20–30 nm, with a passivating oxide coating (<3 nm).

For the microscopy experiments we used marked silicon oxide coated nickel grids. The methanol dispersion was ultrasonicated prior to deposition of the mixture to the grid. To understand the role of thermal stresses on the particles, we heated particles on a hot-stage TEM (Philips CM30) to a temperature of 1173 K. These heating experiments were under vacuum and the particle was continuously monitored during the heating process. In a second set of experiments, several particles were located on the grid with respect to a center marker. The grid was then removed from the microscope and heated in a tube furnace in the presence of air at different temperatures. The grid was then returned to the microscope and the same particles were located with the aid of the marker to observe morphological changes.

In another set of experiments, a recently developed single particle mass-spectrometer (SPMS)<sup>9</sup> capable of quantitative determination of the relative elemental composition of individual nanoparticles was used to determine the temperature for the onset of oxidation in heated air. For these experiments the aluminum nanoparticle/methanol dispersion was aerosolized using dry compressed air. The aerosol stream was passed

\* Corresponding author. E-mail: mrz@umd.edu.

<sup>†</sup> University of Maryland.

<sup>‡</sup> Pusan National University.

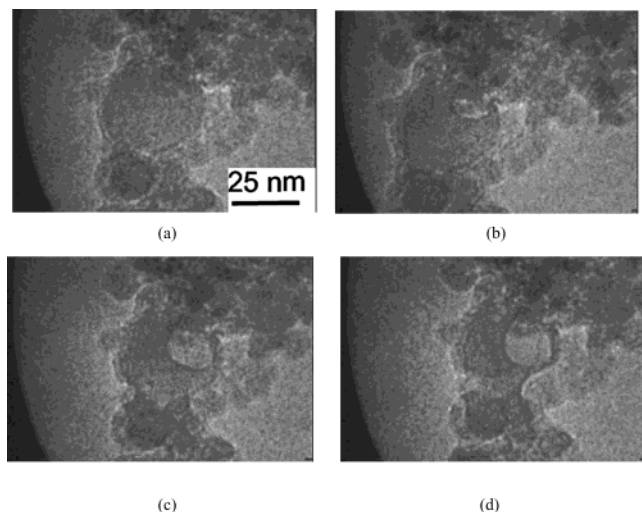


**Figure 1.** Aluminum nanoparticles in vacuum in a hot-stage TEM: (a), (b), (c), and (d) are images taken from a video at about 16.5 min of heating time.

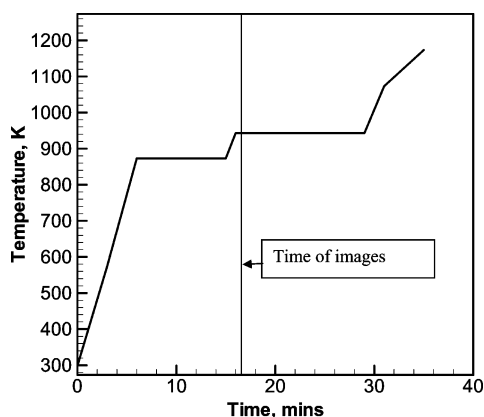


**Figure 2.** Temperature vs time ramp for particle heating in the hot stage of electron microscope.

through several diffusion dryers to remove any methanol that was present in the stream. This stream was then heated to different temperatures, and the particles in the stream were analyzed using the SPMS system following a procedure described in an earlier work.<sup>9</sup>

## Results and Discussions

Figure 1 shows temporal images for the heating of an aluminum nanoparticle in a hot-stage TEM. The temperature ramp employed is showed in Figure 2. All the images were taken at around 16.5 min where major changes were seen to occur and the corresponding temperature was around 940 K, which also happens to roughly correspond to the melting point of bulk aluminum.

In Figure 1a, the oxide shell, which we estimate to be about 3 nm, is still intact, but in Figure 1b the oxide shell has evidently cracked open, and one can clearly see the appearance of a meniscus, which we ascribe to the receding liquid aluminum interface as it flows out of the particles. Figure 1c and 1d shows subsequent stages during this process, which lasts just a few seconds. Using bulk properties as a rough estimate, we note that the density of liquid aluminum ( $2.4 \text{ g/cm}^3$ ) is less than that of solid aluminum ( $2.7 \text{ g/cm}^3$ ), such that when aluminum melts, it expands by 12%. If we neglect the thermal expansion of the oxide shell, which should be negligible at these temperatures, relative to the changes expected for aluminum, then the oxide

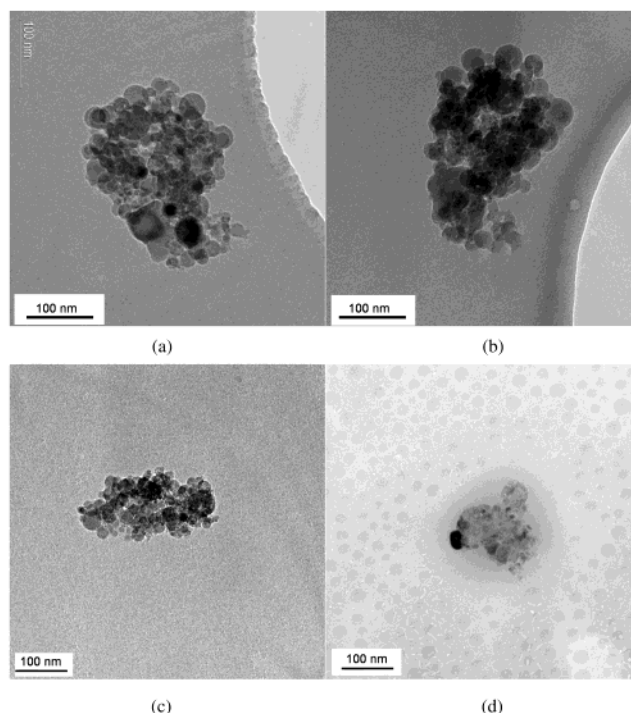


**Figure 3.** Heating of aluminum particles for 10 min at different temperatures in air: (a) and (b) respectively are the images of a particle before and after heating to 873 K; (c) and (d) respectively are the images of a particle before and after heating to 1173 K.

shell will be under tension and the aluminum core under compression. Assuming that the bulk modulus of aluminum ( $\sim 76 \text{ GPa}$ ) can be used at these length scales, we find an internal pressure rise of  $\sim 88000 \text{ atm}$  will be present at the oxide shell due to the density difference. A recent molecular dynamic calculation<sup>11</sup> confirms the presence of a large internal pressure of the aluminum core and negative pressure (tension) of the oxide shell at these elevated temperatures. These results imply that the oxide shell is dynamically unstable upon melting of the aluminum core. These results from molecular dynamics calculations have also shown that the pressure rise in smaller particles is higher than that in larger particles, implying that smaller particles should have a higher propensity to rupture. Also, because of higher curvature, the oxide coating in smaller particles is under higher tension, and hence should rupture with greater ease as compared to the coatings in large particles.

Figure 3 shows the images of two sets of particles, prior to and following heating in air at 873 K (below melting point) and 1173 K (above melting point). In both cases, particles were heated in air for 10 minutes. We observe that the before and after images at 873 K are essentially indistinguishable, while particles heated to a temperature of 1173 K, above the melting point (940 K) of aluminum, clearly show significant restructuring and rupture/loss of distinguishable oxide layer structure. These results are consistent with the hot-stage TEM measurements, but still deal only with the issue of physical restructuring and melting of aluminum and do not address the issue of any chemical change, i.e., oxidation.

To study oxidation as opposed to melting, we use our single-particle mass spectrometer (SPMS) to track the oxygen content of particles under exposure to air at different temperatures. For these experiments, aluminum aerosol had a residence time of about one second in the heated section of the flow reactor.

Figure 4 shows single particle spectra at different temperatures. It can be seen that the first appearance of oxygen in the

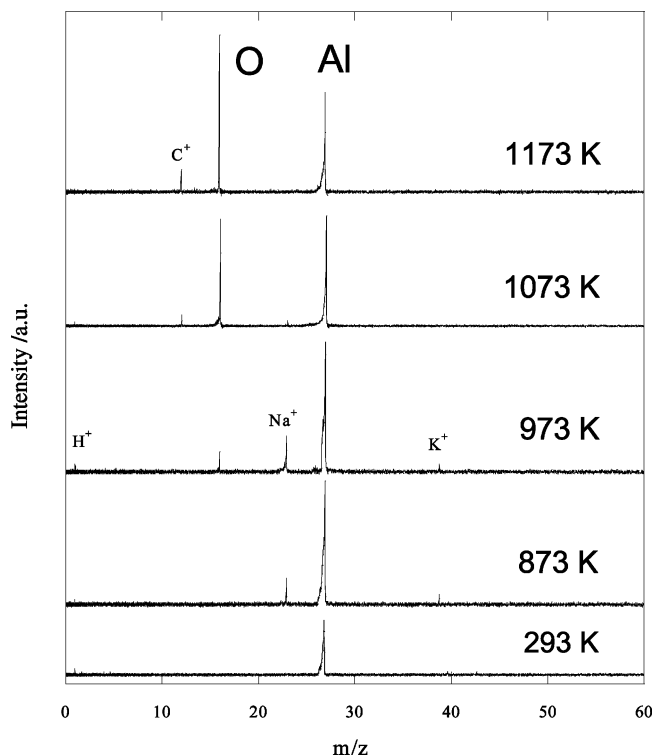


**Figure 4.** Single particle mass spectra for aluminum nanoparticles heated in air at different temperatures.

spectra is not observed until a temperature of 973 K, which is slightly above the melting point of aluminum, while at 100 K lower, no evidence of oxidation is observed. With increasing temperature the oxygen signal intensifies, implying greater extent of oxidation. Prior work with the SPMS for mixed composition or coated particles indicated the sensitivity of about ~1% (mole percentage) in the particle. With 1~2 nm oxide thickness, the SPMS should detect the oxide if it exists. But in these experiments, aluminum dispersed in methanol was used and, unlike the particles used in microscopy experiments, they did not have an initial oxide coating as they were never exposed to ambient atmosphere. In our experimental conditions, the air was mixed with aluminum particles just prior to the furnace and the exposed time for aluminum particles to the air was relatively short (~1 s). Evidently during this period the reactivity of nanoaluminum is sufficiently slow as to preclude the formation of a detectable oxide coating. It is only at a temperature of 973 K that we begin to see the appearance of oxygen in the particle, consistent with the microscopy studies outlined above. Our current work is focused on quantifying the kinetics of oxidation using this experimental approach.

The results of these two very different experiments point to a mechanism whereby the mechanical stability of the oxide shell determines the onset of combustion. As the temperature increases beyond the melting point, the density difference between aluminum solid and liquid causes a rupture in the oxide shell. This results in exposure of aluminum to the oxidizer and subsequent ignition.

Earlier, research groups<sup>8</sup> have reported oxidation of nanoaluminum at temperatures of around 800 K, which is below the

melting point of aluminum. This is significantly different from our observations. These researchers used dynamic thermal techniques such as thermogravimetry. Though these techniques are widely used to measure condensed phase reactions, limitations of these techniques because of uncertainties associated with heat and mass transfer are well known.<sup>9,10</sup> Kinetic measurements of solid-state reactions using both these methods, SPMS and TGA, have been reported,<sup>9</sup> and it has been found that, for example, the onset temperature of thermal decomposition reactions of metal nitrates varied with the variation of mass loading in the case of TGA. In those studies it was observed that the onset temperature was consistently lower with TGA, and that small samples tended to increase the onset temperature. These conventional methods use sample sizes of the order of a milligram, while the SPMS measurement characterizes a single nanoparticle, of the order of a femtogram. It has been reported<sup>12</sup> that the activation energy of a reaction decreases on increase in sample size, and this decrease can result in a lower onset temperature as measured by conventional methods. Other artifacts might include the fact that higher sample size, would result in heat release which raises the temperature of the sample above the measured pan temperature, and therefore an observation of an apparent higher reactivity. The use of a sample size of approximately 1 fg, we believe, mitigates some of these issues and gives a more direct observation of the onset condition to oxidation.

## Conclusion

This letter explores the role of the mechanical stability of the oxide shell over an aluminum nanoparticle and its role in passivating the particle toward oxidation. Experiments were performed using hot-stage TEM imaging and single particle mass spectrometry to explore the morphological and chemical changes, respectively. Results from both experimental approaches support the conclusion that aluminum phase change causes rupture of the oxide shell, and may be the primary initiator in the ignition of aluminum nanoparticles. These results should be of interest to those interested in new propellant formulations based on metal nanoparticles.

## References and Notes

- (1) Merzhanov, A. G.; Grigorjev, Yu. M.; Gal'chenko, Yu. A. *Combust. Flame* **1977**, *29*, 1.
- (2) Breiter, A. L.; Mal'tsev, V. M.; Popov, E. I. *Combust. Explos. Shock Waves* **1977**, *13*, 475.
- (3) Ermakov, V. A.; Razdobreev, A. A.; Skorik, A. I.; Pozdeev, V. V.; Smolyakov, S. S. *Combust. Explos. Shock Waves* **1982**, *18*, 256.
- (4) Lokenbakh, A. K.; Zaporina, N. A.; Knipele, A. Z.; Strod, V. V.; Lepin, L. K. *Combust. Explos. Shock Waves* **1985**, *21*, 73.
- (5) Rozenband, V. I.; Vaganova, N. I. *Combust. Flame* **1992**, *88*, 113.
- (6) Rozenband, V. I.; Afanas'eva, L. F.; Lebedeva, V. A.; Chernenko, E. V. *Combust. Explos. Shock Waves* **1990**, *26*, 13.
- (7) Ivanov, G. V.; Tepper, F. *4th International Symposium on Special Topics in Chemical Propulsion*; Begell House: New York, 1997; p 636.
- (8) Mench, M. M.; Kuo, K. K.; Yeh, C. L.; Lu, Y. C. *Combust. Sci. Technol.* **1998**, *135*, 269.
- (9) Mahadevan, R.; Lee, D. G.; Sakurai, H.; Zachariah, M. R. *J. Phys. Chem.* **2002**, *106*, 11083.
- (10) Ortega, A. *Int. J. Chem. Kinet.* **2001**, *343*, 1.
- (11) Sonwane, C. G.; Mintmire, J. M.; Zachariah, M. R., submitted
- (12) Gallagher, P. K.; Johnson, D. W., Jr. *Thermochim. Acta* **1973**, *6*, 67.